This is a pre-print version of the paper: A pilot-plant for the selective recovery of magnesium and calcium from waste brines. Submitted of Journal Desalination,

A pilot-plant for the selective recovery of magnesium and calcium from waste brines

F. Vassallo[a], D. La Corte[a], N. Cancilla[a], A. Tamburini[a,b], M. Bevacqua[b], A. Cipollina*[a, b], G. Micale[a,b]

[a]*Dipartimento di Ingegneria, Università degli Studi di Palermo (UNIPA)- viale delle Scienze Ed.6, 90128 Palermo, Italy.*

[b]*ResourSEAs SrL, viale delle Scienze Ed.16, 90128 Palermo, Italy.*

*corresponding author: andrea.cipollina@unipa.it

Abstract

The problem of brines disposal has raised great interest towards new strategies for their valorisation through the recovery of minerals or energy. As an example, the spent brine from ion exchange resins regeneration is often discharged into rivers or lakes, thus impacting on the process sustainability. However, such brines can be effectively reconcentrated, after removal of bivalent cations, and reused for the resins regeneration. This work focuses on developing and testing a pilot plant for selective recovery of magnesium and calcium from spent brines exploiting a novel proprietary crystallization unit. This is part of a larger treatment chain for the complete regeneration of the brine, developed within the EU-funded ZERO BRINE project. The pilot crystallizer was tested with the retentate of the nanofiltration unit processing the spent brine from the industrial water production plant of Evides Industriewater B.V. (Rotterdam, The Netherlands). Magnesium and calcium hydroxide were selectively precipitated by adding alkaline solution in two consecutive steps and controlling reaction pH. Performance was assessed in terms of recovery efficiency and purity of produced crystals, observing in most investigated cases a recovery of about 100% and 97% and a purity above 90% and 96%, for magnesium and calcium hydroxide, respectively.

Keywords: *Magnesium hydroxide, critical raw materials, valorisation, waste brine, reuse, circular.*

1. Introduction and literature review

The rapid growth of global population and industrialisation, coupled with the continuous search for novel and more sustainable sources of raw materials pushes the scientific and technological community towards the analysis of circular economy approaches for the valorisation of industrial streams via recovery of valuable materials and water. With this respect, several industrial processes nowadays generate brines, whose disposal arises environmental concerns, such as the increase of salinity, discharge of chemical used for pre-treatment and heavy metals etc [1,2], due to the high concentration of dissolved minerals (mainly sodium (Na), potassium (K), magnesium (Mg), Calcium (Ca) and chloride (Cl)), with a total dissolved solid (TDS) up to around 80 g/L, altering the ecosystem of the receiving water bodies [3,4]. Therefore, interest is rising towards a variety of waste industrial brines in order to exploit them as an alternative source of minerals and, at the same time, reducing/avoiding the discharge of the brine into a body water and then the environmental impact [5,6]. Among the cations present in the waste brine, magnesium is one of the most valuable. In fact , this has been defined as one of the twenty critical raw materials (CRM) by the European Commission, because more than 96% of the magnesium used in European countries is imported [7] causing a high risk of supply interruption [8].

There are many industrial sectors, which produce waste brines, namely: (i) mining industry, (ii) sea and brackish water desalination, (iii) industrial water softening plants, etc.

Regarding the waste brine produced by the mining sector (i), Poland is the European country with the largest number of active coal mines. These coal mines produce about 550 m^3 per day of waste brines, containing about 0.3-0.4 g/l of magnesium [9], which are directly discharged in rivers [10]. In order to minimize the environmental impact and recover magnesium, Turek and Gnot studied the possibility to recover magnesium hydroxide (used for the refractories industries) as by-product from a two-stage system that treated waste brines [11]. In particular, they added NaOH, as alkaline reactant, to recover magnesium as magnesium hydroxide to avoid the co-precipitation of calcium. With reference to a similar case study, Micari et al. [12] performed a theoretical techno-economic analysis demonstrating that an integrated treatment chain can effectively lead to the circular recovery and reuse of chemicals such as $Mg(OH)_2$, $CaCO_3$ and NaCl in addition to fresh water.

Another important industrial process, which produces very large amounts of waste brines, is seawater desalination (ii). Typically, the desalination brine has a salinity 1.5-2 times higher than

seawater (TDS of 35 g/L), with larger values for the widely adopted reverse osmosis (SWRO) process [13–15]. In 2019, Jones et al analysed the operation of 15,906 RO desalination plants, covering 81% of the total number of desalination plants and with a total desalination capacity equal to 34.81 billion m^3/y, estimating a waste brine production around 51.7 billion m^3/y [14]. Different strategies were investigated to manage the produced waste brine depending on the location of the desalination plant. Commonly, desalination plants are located near the sea, so the direct discharge in receiving water bodies (e.g. seas and oceans) is presently the most common disposal strategy. In order to reduce the environmental impact, different mitigation strategies have been considered, e.g.: (i) brine mixing with power plant cooling water [1,16], (ii) single pipe discharge to deep water [1], (iii) discharge pipe equipped with diffusers [1,3].

On the other hand, in the case of inland brackish water desalination plants far from the sea, other disposal strategies have been studied, namely: (i) deep well injection [5,17–19], (ii) disposal into surface water bodies [20], (iii) irrigation of plants tolerant of high salinity [17,21,22], (iv) direct discharge in the municipal wastewater treatment plant (waste brine has to be 20 times less than the capacity of the treatment plant) [22,23] and (v) disposal into evaporative ponds and periodically the precipitated minerals are disposed in landfills. All disposal methods presented are feasible for low production and without the presence of any hazardous chemical content, although they are subject to restrictions dictated by climatic conditions, seasonal demand, land availability and groundwater conditions [24].

These strategies for the disposal of waste brine are often unsustainable due to (i) high disposal cost, ranging from 5% to 33% of the total cost of desalination, and (ii) environmental impact [24]. A valuable alternative to the direct disposal is the minimization of the brine volume. The minimization strategy can be performed via membrane-based technologies, such as electro-dialysis [25], forward osmosis (FO) [25–29], pressure retarded osmosis (PRO) [30], or thermal-based technologies, such as Wind Aided intensive eVaporation [31], multi effect distillation (MED) [32], multi stage flash (MSF) [15], or hybrid thermal-membrane based technologies, i.e. membrane distillation (MD) [33,34]. The minimization techniques allow to decrease the final volume of waste brine for disposal, thus reducing the environmental issues and the costs associated with disposal. However, a combination of minimization and evaporative techniques (e.g. evaporative ponds) avoiding the direct disposal of waste brine and recovery of useful salts mixtures, following the Zero Liquid Discharge (ZLD) concept [34,35].

Another example of waste brine generating process is given by the water softening industry (iii), where highly concentrated NaCl solutions are often adopted for the regeneration of the Ionic Exchange resins (IEXs). After the regeneration step, the disposal of the spent regenerant solution, still rich in sodium chloride, but also in magnesium and calcium ions, may cause environmental issues due to the high salinity of large volumes produced. Flodman and Dvorak [37] suggested some strategies to reduce the salts consumption during the regeneration. They proposed a regeneration system where the spent brine is partially recycled and mixed with the fresh regeneration solution in order to reduce the consumption of the salts and the disposal of the spent brine, although at the expense of an increased frequency of the regeneration cycles of the resins. Chen et al [38] proposed an alternative closed loop regeneration system, through which disposal of regeneration solution is avoided. The regeneration system consists of a bipolar membrane electrodialysis unit (BMED) and a crystallizer. The BMED was used to restore the acids and alkaline solution used for the regeneration of weak acid cation resins and to recover calcium and magnesium [38]. Very recently, Micari et al. [39,40] performed a techno-economic analysis of a treatment chain for the regeneration of IEX spent brines, demonstrating the feasibility of the process leading to the full regeneration of NaCl regenerant solution and the production of marketable by-products such as $Mg(OH)_2$ and $Ca(OH)_2$. The core of the chain is a selective crystallizer for the quantitative recovery/removal of magnesium and calcium in the form of hydroxides. This has been demonstrated at a pilot scale.

The present work focuses on the development of a selective precipitation pilot plant for the removal and recovery of bivalent metals hydroxide (Mg and Ca), which makes use of a novel proprietary crystallization unit [41]. It is interposed within the above mentioned treatment chain, with the aim of valorising spent brines produced by the regeneration of IEX resins for water softening, the process system is installed at the premises of Evides Industriewater B.V., in Rotterdam (The Netherlands), developed within the framework of the EU-funded project "*ZERO BRINE"*[42] (aiming at proposing new solutions to treat different types of waste industrial brines with a circular approach). A schematic representation of the whole treatment chain is shown in Figure 1.

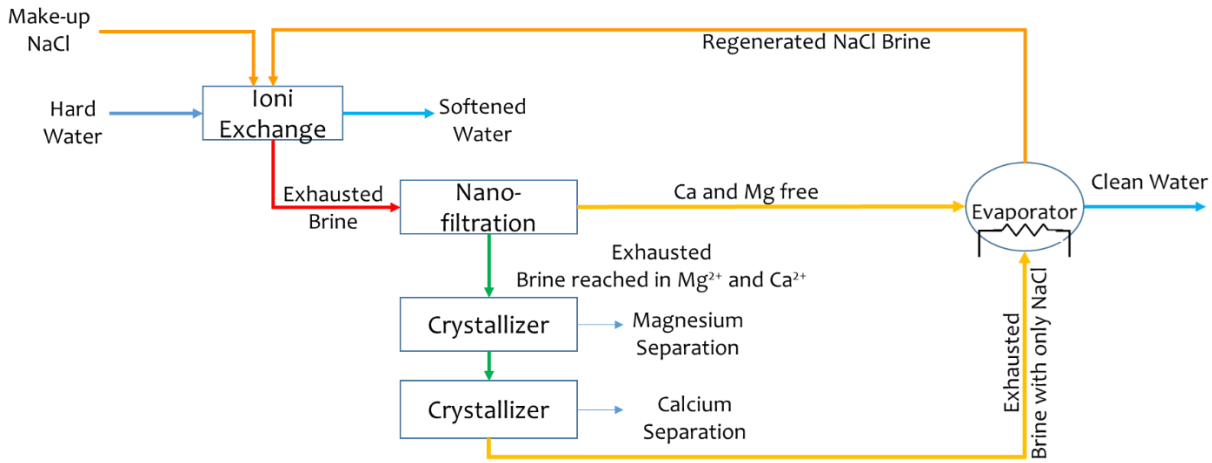

Figure 1.Schematics of the treatment chain proposed within the *ZERO BRINE* EU-H2020 project for the valorization of brines from IEXs water softening plants.

The whole process consists of the following units: (i) nano-filtration (NF), (ii) Mg & Ca crystallization and (iii) multi effect distillation (MED). The waste brine from IEX is fed to an NF unit, which produces a retentate enriched in bivalent ions, e.g. magnesium and calcium, and a permeate enriched in monovalent ions, such as sodium chloride. Afterwards, the retentate is fed into a two-step crystallizion for selective removal and recovery of magnesium and calcium hydroxide, by chemical precipitation using an alkaline solution. After separating the hydroxide slurry, within a continuous drum filter, the clarified brine (almost Ca- and Mg-free) is neutralized to pH≈7 by addition of hydrochloric acid and mixed with the permeate from the NF. This stream is eventually fed into the MED unit in order to further concentrate the solution of sodium chloride, thus reaching the target value suitable for reuse in the IEX regeneration step.

This paper presents the assembly and testing of the selective crystallization pilot plant including the results of a wide experimental campaign carried out in the Netherlands (Plant One B.V., Botlek, Rotterdam). The research allows evaluating the pilot plant performance in terms of operational, stability, recovery/removal efficiency and solid products purity.

2. Pilot Facility and operational procedures

2.1 Description of Mg/Ca fractionated reactive crystallization concept

The fractionated crystallization of the two Mg and Ca hydroxides is achieved by careful control of the reaction pH. To this aim, a preliminary test was performed using a laboratory semi-batch reactor and the following experimental procedure:

- an artificial solution, prepared using magnesium chloride hexahydrate (VWR, purity >99%), calcium chloride dehydrate (Honeywell, purity >99%) and sodium chloride (Sale di Volterra, purity >99%) in deionised water, was used to reproduce the typical composition of the IX spent brine (see Table 1);
- the artificial brine was placed inside a magnetically stirred beaker, where a NaOH solution was slowly added at constant rate (60 mL/h) via a syringe pump.

The pH was monitored by a portable pH-meter (WTW, mod. 3320) and the obtained pH trend over the time is shown in Figure 2.

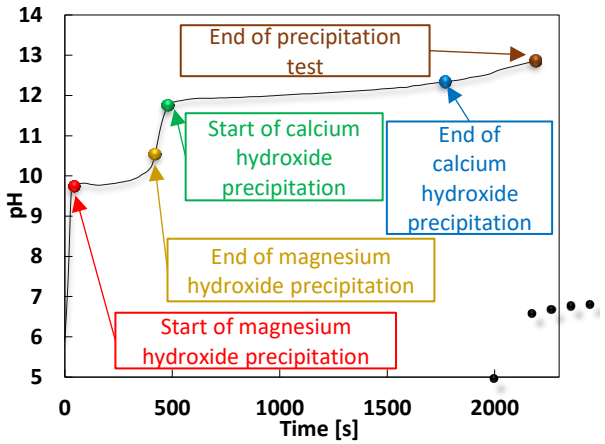

Figure 2 Precipitation path for the recovery of magnesium and calcium hydroxide

Starting from a pH value near 6, the 1M NaOH solution is slowly injected, and the pH increases quickly until a value around 9.8 (red point in Figure 2) is achieved, when the precipitation of magnesium hydroxide begins. Then, the pH increases very slowly to 10.4 (orange point in Figure 2), where magnesium can be assumed to be quantitatively precipitated. The produced magnesium hydroxide slurry is then filtered and the solids are dried and analysed. Meanwhile, the Mg-free filtered solution (after being analysed) is fed again to the batch reactor for the second precipitation

step along with a 4M NaOH solution. Also in this case, the experimental procedure was the same described above for the precipitation of $Mg(OH)_2$. Again, the pH increases quickly until a value of 11.75 (green point Figure 2), where the precipitation of calcium hydroxide starts. Afterwards, the pH increases slowly reaching a value near 12.4 (blue point in Figure 2), where, theoretically, all calcium is precipitated as calcium hydroxide. The test was extended until a pH of near 13 (brown point in Figure 2) was achieved in order to ensure that Ca is quantitatively precipitated. After this second precipitation step, the slurry was filtered to separate and analyse solids and clarified solution.

The cations composition of the initial brine and of the two clarified solutions are reported in Table 1, along with the purity of two solid hydroxides obtained. A quantitative precipitation of both cations and a purity of the solids above 98% is obtained, thus confirming the possibility to quantitatively recover magnesium and calcium hydroxide at high purity, matching the specifications required by the market.

Table 1. Fed batch test: ionic composition, crystallisation reaction conversion and purity of magnesium and calcium hydroxide

	Na^+ [g/L]	Ca^{2+} [g/L]	Mg^{2+} [g/L]	Cl^- [g/L]	pH
IXE Spent Brine	26.15	24.12	3.08	91.98	6.0
1° step (filtrate)	25.51	22.53	0.02	73.37	10.4
2° step (filtrate)	39.41	0.00	0.00	58.02	13.0
$Mg(OH)_2$	Purity			>98%	
	Precipitation yield			>99%	
$Ca(OH)_2$	Purity			>98%	
	Precipitation yield			>99%	

Following the results described, a conceptual scheme of a continuous system for fractionated precipitation of Mg and Ca hydroxides is shown in Figure 3, consisting of:

(a) brine storage tank;

(b) precipitation unit where magnesium, firstly, and calcium, secondly, are precipitated from the brine by direct mixing with a sodium hydroxide solution ("precipitation unit"), represented as two separate blocks in the diagram, though being the same unit in practice.

(c) Magnesium and Calcium settling tanks are used, to collect and settle the produced slurry in order to prepare a concentrated slurry to be sent to the filtration unit.

(d) filtration unit, where solids particles are separated from the slurry ("filtration unit").

(e) intermediate storage tank, where the first step clarified solution is stored before feeding the 2nd step precipitation for Calcium recovery;

(f) neutralization unit, which allows for the neutralisation of the clarified solution exiting from the 2nd step settling tank and Ca-slurry filtration.

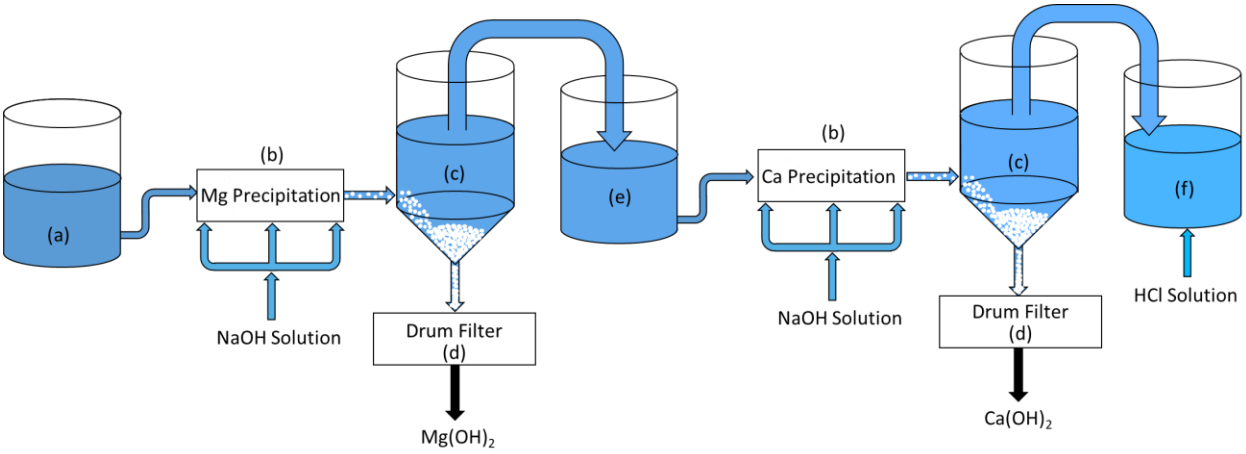

Figure 3.Conceptual scheme of the crystallisation pilot plant. (a) Storage tanks, (b) Precipitation Unit, (c) Settling tank, (d) Filtration unit, (e) Intermedia tank, (f) Neutralization unit

2.2 Description of the pilot plant

The pilot system is divided into three main sections:

1. Precipitation section, consisting of the proprietary Multiple-Feed Plug Flow Reactor (MF-PFR) [41], and relevant auxiliary devices (e.g. pumps, tanks and sensors);
2. Filtration section, consisting of the drum filter and relevant auxiliary devices;

3. Neutralization section, consisting of a pH control loop with relevant pumps, sensors and tanks.

A simplified Piping and Instrumentation Diagram (P&ID) including the three sections is reported in Figure 4.

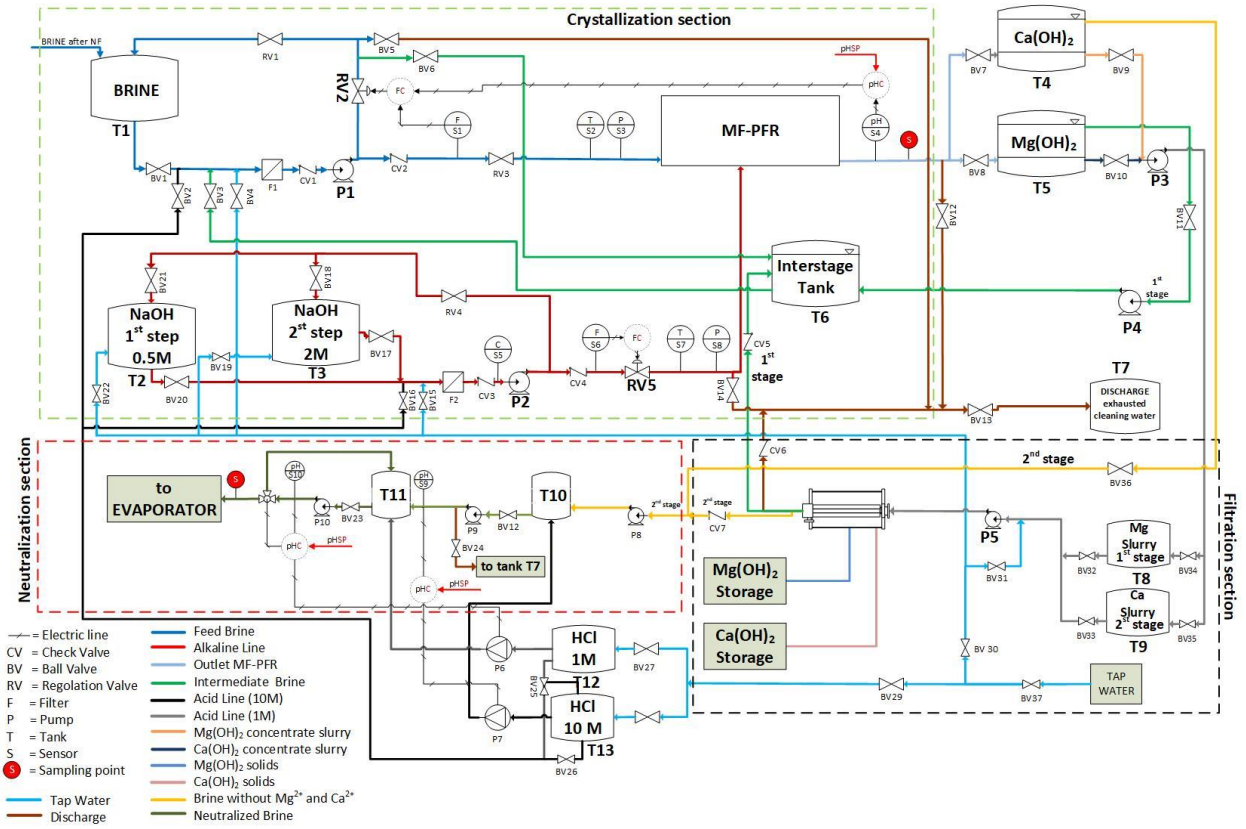

Figure 4. Simplified P&I Diagram of the pilot plant.

2.2.1 Precipitation Section

The main unit of the precipitation section is the Multiple Feed Plug Flow Reactor (MF-PFR) [41]. In this unit, the brine is injected in the vessel using multiple distributed holes, whose position and orientation have been purposely selected in order to promote fast mixing of reactants. With reference to the P&ID shown in Figure 4, the operation of the unit can be described as follows.

The tank *T1* is filled with brine from the Nano Filtration unit, while tanks *T2* and *T3*, are filled with sodium hydroxide solutions used as reactant for the two steps of Mg- and Ca- precipitation. Brine and alkaline solutions are pumped by magnetic drive centrifugal pumps (IWAKI, mod. MD-

40RZ-220N and MD-30RZ-220N, respectively). Both pumps are equipped with a recycle loop to better control flow-rates, using two electric-motorized valves (FIPNET, mod. VDK/CE). Flow-rates are measured by magnetic induction flow-meters (KHRONE, mod. OPTIFLUX 4300 C, calibrated for a measuring range of 0-8 L/min and 0-4 L/min, respectively). Inlet pressure is measured by pressure transducers (Krohne, mod. OPTIBAR P1010C and Vega, mod. VegaBar 14 respectively), in order to monitor the pressure drops inside the annular and internal sections of the reactor. Temperature is measured by Pt100 sensors (KHRONE, mod. TRA-C20).

The direct mixing of brine and alkaline solutions inside the MF-PFR reactor leads to the precipitation of $Mg(OH)_2$ crystals in the form of agglomerates, which exit from the reactor with the outlet slurry.

As discussed above, for effective operation it is crucial to control the pH of the slurry exiting the MF-PFR. To this aim, a pH-Meter (KHRONE, mod. PH 8320) was used for the measurement.

A picture of the MF-PFR prototype is reported in Figure 5.

Figure 5. A picture of the novel proprietary crystallization reactor tested at the Brine Excellence Center laboratory of University of Palermo (a), then installed and operated at the premises of Plant One (Botlek, Rotterdam, NL) (b).

Following the precipitation of magnesium hydroxide, the produced slurry is stored in a settling tank (*T5*). The settled slurry is sent to the storage tank (*T8*), ready for filtration, while the clarified solution is sent to the intermedium storage tank (*T6*) to be further processed for the removal of Ca as $Ca(OH)_2$ in a second precipitation step.

Calcium hydroxide is precipitated according to the same steps, though a higher pH is maintained, and a different settling tank is adopted (*T4*). From this, the clarified solution is sent to the tank (*T10*) for neutralization, while the settled slurry is sent to the storage tank (*T9*), ready for filtration. The clarified solution is circulated by two membrane pumps (Shurflo, mod. SH-2088-443-144) working in parallel.

The reactor is periodically cleaned using a $10\%_{w/w}$ hydrochloric acid solution, in order to dissolve residual scaling, and then flushed with tap water.

2.2.2 Filtration Section

The main unit of the filtration section is a vacuum drum Filter, Figure 6.

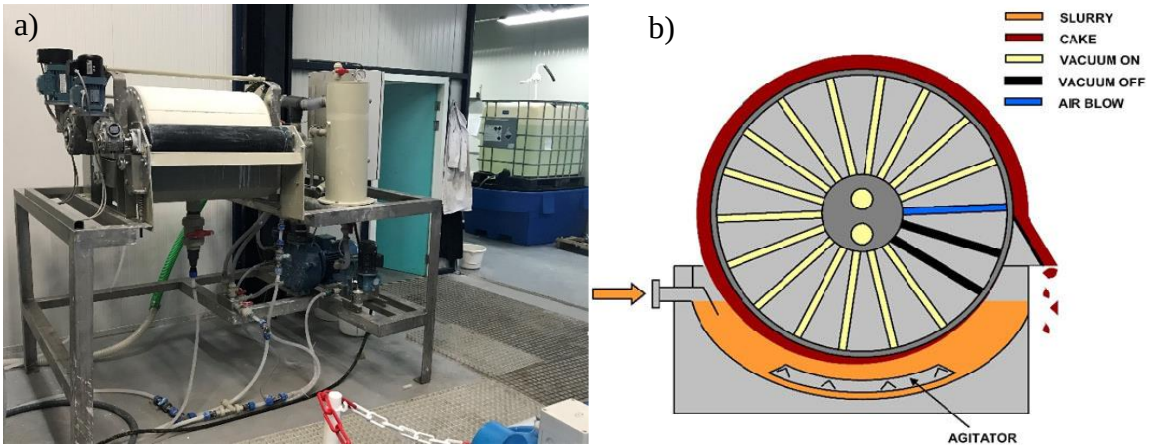

Figure 6.a) Picture of the drum filter installed and operated at the premises of Plant One (Botlek, Rotterdam, NL). b) Conceptual scheme of operation of a drum filter [43]**.**

The vacuum drum filter, provided by WesTech, consists of the following parts:

- Feed tank, which is filled with the concentrated slurry. Inside the tank, there is an agitator necessary to maintain the solids in suspension.
- Rotating vacuum drum, with a filtration cloth of 1 m^2 filtration area. The vacuum drum is split into 12 sectors, as shown in Figure 6.*b*, some of them kept under vacuum and others at atmospheric pressure. A part of the vacuum drum is submerged inside the slurry, allowing the submerged sectors to suck the solution from the concentrated slurry. The unsubmerged sectors are used for washing the cake collected on the surface of the cloth, then, for drying the crystals and, finally, for the detachment of the cake (sector at atmosphere pressure).

- Two receiving tanks, one for collecting the sucked solution and the other for collecting the washing water. The two tanks are connected to the vacuum drum by means of a tailored perforated Teflon dish, which allows connecting some sectors of the vacuum drum with a specific receiving tank. A vacuum pump (Robuschi, mod RVS_16/M-06) generates the vacuum inside the two tanks, while two peristaltic pumps (Ragazzini srl, mod. PSF2 and mod. PSF3) allow for the extraction of sucked solution and cleaning water from the tanks to the outlet collecting basins.
- Spray nozzle distributors, which spray the cleaning water on the top of the drum filter investing the whole surface of the cake.

The concentrated slurry feeding the filtration unit is stored in tanks *T8* and *T9* and is circulated by means of a membrane pump (SHURFLO, mod. SH-2088-594-444).

The filtered solution is then directed to the intermedium storage tank (*T6*), in case this has to be fed to the calcium precipitation step, or to the neutralization section, when all bivalent ions have been precipitated.

Figure 7 shows a picture of the magnesium hydroxide cake obtained from filtration.

Figure 7. a) Magnesium cake on the filter cloth surface and b) detached magnesium hydroxide in the collection tray.

2.2.3 Neutralization section

The neutralization of clarified and filtered brine (arriving from tank *T4* and from the second filtration step, respectively) is carried out via two subsequent steps, which allows maintenance of finely tuned control of pH [44]: (i) the brine is mixed with a 10M hydrochloric acid solution in order to neutralize the 90% of hydroxide ions, and, then, (ii) the brine is mixed with a 1M acid solution to finalize the neutralization.

The neutralized brine pH is measured by means of an inline pH-meter (KHRONE, mod. PH 8320).

2.3 Auxiliary units.

All sub-sections of the pilot plant unit were connected using welded rigid polypropylene (PP) pipes and fittings. Also, all valves are made of PP, in order to be perfectly resistant to the highly aggressive brine and solutions of sodium hydroxide and hydrochloric acid [45].

Pipes and instrumentation of the MF-PFR were installed on a support structure built with corrosion-resistant materials (aluminium-profiled bars and PVC sheets).

The external connections (FO from brine tanks, filtration unit and intermediate buffer tanks) have been constructed using semi-rigid PE tube, fittings and valves.

Information on all tanks adopted in the pilot plant is reported in Table 2.

Table 2. Tanks used in the pilot plant.

Tank n.	volume [L]	material	used for
T1	5000	LLDPE	Collecting the Brine from Nano-filtration step
T2	1000		Storing the NaOH aqueous solution for precipitation of $Mg(OH)_2$
T3			Storing the NaOH aqueous solution for precipitation of $Ca(OH)_2$
T4	1000	HDPE	Collecting and settling the $Mg(OH)_2$ slurry
T5			Collecting and settling the $Ca(OH)_2$ slurry
T6	3000	LLDPE	Collecting the free Mg brine for the second step
T7			Collecting the waste effluents of the MF-PFR and the drum filter
T8	300	PE	Collecting the $Mg(OH)_2$ concentrated slurry
T9	300	PE	Collecting the $Ca(OH)_2$ concentrated slurry
T10	1000	HDPE	First step of neutralization
T11	5000	LLDPE	Second step of neutralization

T12	200	HDPE	Storing 1 M of hydrochloric acid
T13			Storing 1 M of hydrochloric acid

2.4 Pilot plant operational procedures

The start-up of the MF-PFR unit requires up to 10-15 minutes in order to stabilize flow rates and pH value of the produced slurry. After steady-state conditions are reached, the system maintains a very stable behaviour (as reported in Figure 9).

The start-up of the drum filter requires a longer transient time (0.5-1 hours) needed for the formation of the solids cake on the cloth surface (about 2-3 mm of thickness allows the cake to be easily discharged continuously). Following the start-up, also the drum filter can operate in a stable behaviour for hours.

Similar start-up and operating procedures are adopted for the two precipitation steps of $Mg(OH)_2$ and $Ca(OH)_2$.

2.5 Sampling and analytical procedures

Samples for analytical characterisation were taken at steady-state operation (typically every 3-4 hours of operation), with a volume of 1 litre of suspension collected from the outlet of the MF-PFR.

The samples were filtered in a laboratory vacuum filtration system. The filtered solution was stored and analysed by means of ion chromatography (IC, Metrohm 882 Compact IC plus). The filtered solids were washed, then dried in an oven at 120°C for 12h. All samples were analysed by IC after dissolution with HCl and dilution with deionised water. Some of the $Mg(OH)_2$ samples were also analysed by X-Ray Diffraction (XRD, Pan Analytical Empyrean) in order to determine whether $CaCO_3$ co-precipitated with $Mg(OH)_2$.

2.6 Definition of main reaction performance parameters

The following operating/performance parameters were monitored and used to evaluate the behaviour of the system:

- pH: related to the reaction conversion, mainly used to control the fractionated crystallisation of $Mg(OH)_2$ in the first precipitation step and the Ca removal in the second step;
- Magma density (M_T): indicating the solids concentration in the suspension, calculated from the measured weight of the filtered solids (m_s) and the filtrate volume (V_f):

$$\boldsymbol{M_T = \frac{m_s}{V_f}} \quad \textbf{(1)}$$

- Purity of solids: it expresses the percentage of Mg^{2+} (or Ca^{2+}) ions with respect to the total amount of cations measured via the IC analysis:

$$\boldsymbol{Purity = \frac{C_{Mg^{2+}} (\, or\, C_{Ca^{2+}})}{\sum_{j=1}^{N} C_i}} \quad \textbf{(2)}$$

- Recovery (Y): it expresses the recovery efficiency in the crystallisation step. Computed as the ratio between precipitated Mg (or Ca) and total amount of magnesium (or calcium) present in the feed:

$$\boldsymbol{Y = \frac{N_i^o - N_i}{N_i^o}} \quad \textbf{(3)}$$

Where *N* is the molar flow-rate, the apex *o* refers to the initial mole-flow rate, while subscript *i* refers to the considered cation, *i.e.* Mg^{2+} or Ca^{2+}.

2.7 Experimental tests

Long-run experiments (8 hours) were carried out with 3 different classes of feed brines resulting from three different phases of IEXs regeneration: i) Standard (Std), resulting from the averaging effect of the IEXs outlet buffering storage tank, where spent regenerant is stored; ii) Low, resulting from the final phase of the IEX regeneration (lower bivalent concentration); and iii) High, resulting from the peak phase of releasing bivalent ions in the spent regenerant. The first condition was mostly adopted and 9 different feed brines from IEXs outlet storage tank were utilised, thus generating a high variability of ions concentration with respect to the std average values (see Table 3 and Figure 8). In Table 3, the average composition of three different tested brines are reported. On the other hand, only 2 spot tests were conducted with the Low and High feed brine. Figure 8 reports the average concentration of the main cations and anions in the tested brines, also indicating the range of variability of concentration for the std brine.

Table 3.Average composition of the 3 classes of feed brine adopted for the precipitation tests (measured deviation from average value is reported between brackets for *case B*).

Brine coming from NF	*pH*	*Conductivity [mS/cm]*	*TDS [g/L]*	*Concentration of main cations in solution [g/L]*				*Concentration of main anions in solution [g/L]*		
				Na^+	K^+	Ca^{2+}	Mg^{2+}	HCO_3^-	Cl^-	SO_4^{2-}
A(Low)	*7.2*	*50.1*	*26.5*	*4.74*	*0.15*	*8.3*	*1.02*	*0.29*	*16.0*	*0.17*
B (Std)	*7.0*	*74.2 (±21.0)*	*60.3 (±21.7)*	*8.01 (±2.9)*	*0.21 (±0.07)*	*12.1 (±5.0)*	*1.60 (±0.5)*	*0.12 (±0.04)*	*37.8 (±14.8)*	*0.54 (±0.57)*
C(High)	*7.0*	*91.4*	*81.6*	*11.49*	*0.24*	*15.8*	*2.00*	*0.14*	*51.4*	*0.65*

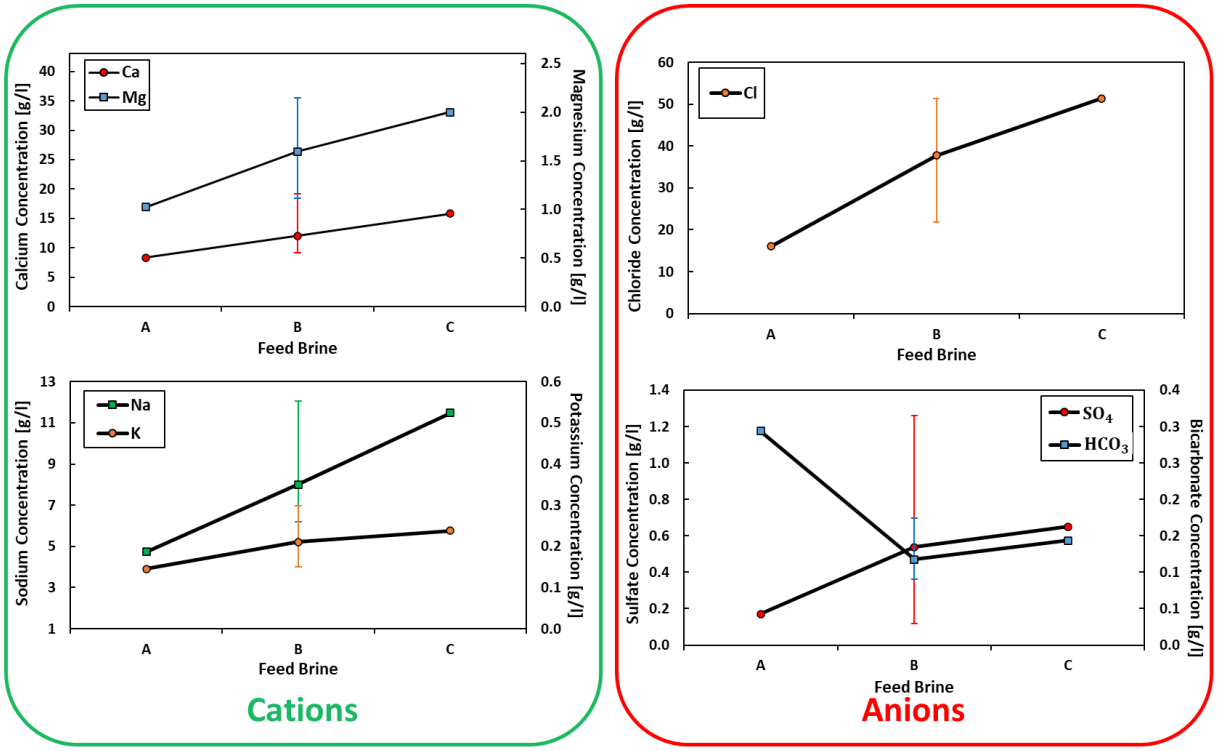

Figure 8. Average concentration of ions in the 3 classes of feed brines. For case B (std) the bars indicate the spanning range of concentration in all brines tested.

All long-run experiments were performed with the aim of analysing the stability and robustness of the pilot in terms of inlet flow rate, outlet pH and system's performance parameters, as discussed in section 2.6. In the following Table 4 and Table 5 details of operating conditions for all the experiments are reported.

Table 4. Operative conditions for $Mg(OH)_2$ crystallisation experiments .

Test run ID	*pH*	*Operative Condition of system*[*]				
		Brine Flow Rate [L/min]	*NaOH Flow Rate [L/min]*	*NaOH Conc. [mol/L]*	*Produced slurry [L]*	*Worked Hours [h]*
A (Low)	*10.5*	*2.45*	*0.17*	*0.50*	*1000*	*6.5*
B1 (Std)	*10.6*	*2.0*	*0.41*	*0.40*	*900*	*7.0*
B2 (Std)	*10.6*	*2.1*	*0.4*	*0.40*	*500*	*3.3*
B3 (Std)	*10.7*	*2.0*	*0.37*	*0.40*	*550*	*4.0*
B4 (std)	*10.7*	*2.0*	*0.37*	*0.40*	*450*	*3.3*
B5 (Std)	*10.6*	*1.2*	*0.45*	*0.40*	*800*	*8.5*
B6 (Std)	*10.5*	*1.3*	*0.46*	*0.40*	*900*	*8.7*
B7 (Std)	*10.5*	*1.2*	*0.42*	*0.40*	*800*	*8.5*
B8 (Std)	*10.35*	*2.7*	*0.38*	*0.50*	*700*	*4.0*
B9 (Std)	*10.8*	*1.6*	*0.4*	*0.50*	*1000*	*8.5*
C (High)	*10.25*	*6.1*	*0.34*	*1.00*	*500*	*1.5*

[*] pH was measured with an accuracy of ±0.1; flow rates were measured with an accuracy of ±0.02 L/min; NaOH concentration was measured with an accuracy of ±0.02M.

Table 5. Operative conditions for $Ca(OH)_2$ crystallisation experiments.

Test run ID	*pH*	*Operative Condition of system*[*]				
		Brine Flow Rate [L/min]	*NaOH Flow Rate [L/min]*	*NaOH Conc. [mol/L]*	*Produced slurry [L]*	*Worked Hours [h]*
A (Low)	*13.2*	*1.36*	*0.33*	*4.0*	*750*	*7.5*
B1 (Std)	*13.0*	*1.4*	*0.36*	*2.0*	*650*	*6.2*
B3 (Std)	*13.1*	*1.4*	*0.38*	*2.0*	*900*	*8.5*
B5 (Std)	*13.1*	*1.3*	*0.42*	*2.0*	*800*	*8.0*
B7 (Std)	*13.0*	*1.2*	*0.45*	*2.0*	*850*	*8.5*
B8 (Std)	*13.1*	*1.56*	*0.36*	*4.0*	*800*	*6.0*
B9 (Std)	*13.3*	*1.21*	*0.3*	*4.0*	*550*	*6.2*
C (High)	*13.1*	*1.45*	*0.32*	*4.0*	*500*	*5.0*

[*] pH was measured with an accuracy of ±0.1; flow rates were measured with an accuracy of ±0.02 L/min; NaOH concentration was measured with an accuracy of ±0.07M.

3. Results and Discussion

3.1 System stability in long-run operation

During the long-run pilot test, all relevant operative parameters were recorded and plotted against time to assess the system stability and the robustness.

For the sake of brevity, only results relevant to one case (B5) are shown in Figure 9.a, for magnesium precipitation, and in Figure 9.b, for calcium precipitation, since the plots for all the other tests performed are very similar to these ones.

The test-run can be divided in three main phases: (i) start-up, (ii) steady-state operation, (iii) shutdown and cleaning. During the start-up, brine and the alkaline flow-rates are adjusted in order to reach the required optimal reaction pH. Once this condition is reached, the pilot works at steady-state for about 7-8 hours. At the end of the run, the reactor is cleaned by flushing 10%$_{w/w}$ hydrochloric acid solution for a few minutes in the brine and alkaline circuit, in order to dissolve possible magnesium or calcium hydroxide scaling inside the reactor, and, subsequently, flushed with tap water for about 10 minutes.

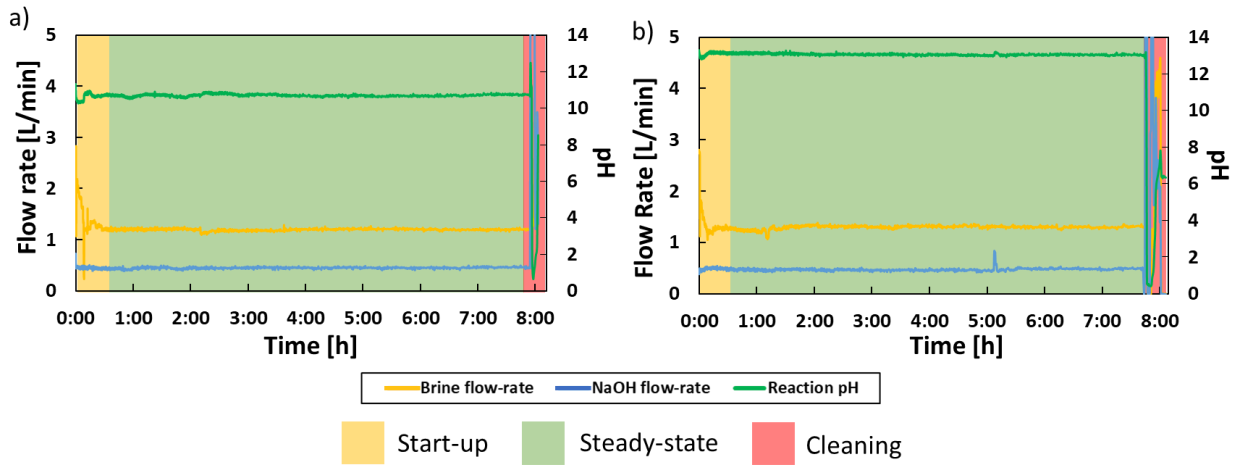

Figure 9.Variation of the outlet pH and both inlet flow rates vs experimental time. a) Precipitation of magnesium hydroxide, and b) precipitation of calcium hydroxide.

As shown in Figure 9, the reaction pH and both flow rates were very stable during steady-state operation, which highlights the robustness of the pilot unit once the stationary-condition is reached.

It is worth mentioning that stable operations were maintained also thanks to some control actions required in order to minimize the effects of disturbances on the flow rates, such as the increase of pressure drops due to nozzles scaling, or the variation of level in the feed tanks. However, control actions were smooth and perfectly feasible within the nominal operation of the system.

In addition, some small control actions were needed in order to compensate for slight variations in Mg and Ca concentration in the feed brine, likely caused by time-dependent stratification phenomena within the feed tanks.

3.2 Performance of the reactive precipitation processes

3.2.1 Magnesium hydroxide precipitation step

Solid purity and recovery efficiency for the tests $Mg(OH)_2$ precipitation are reported in Figure 10. Magnesium and calcium concentration in the feed brine and magma density are also reported to support the results.

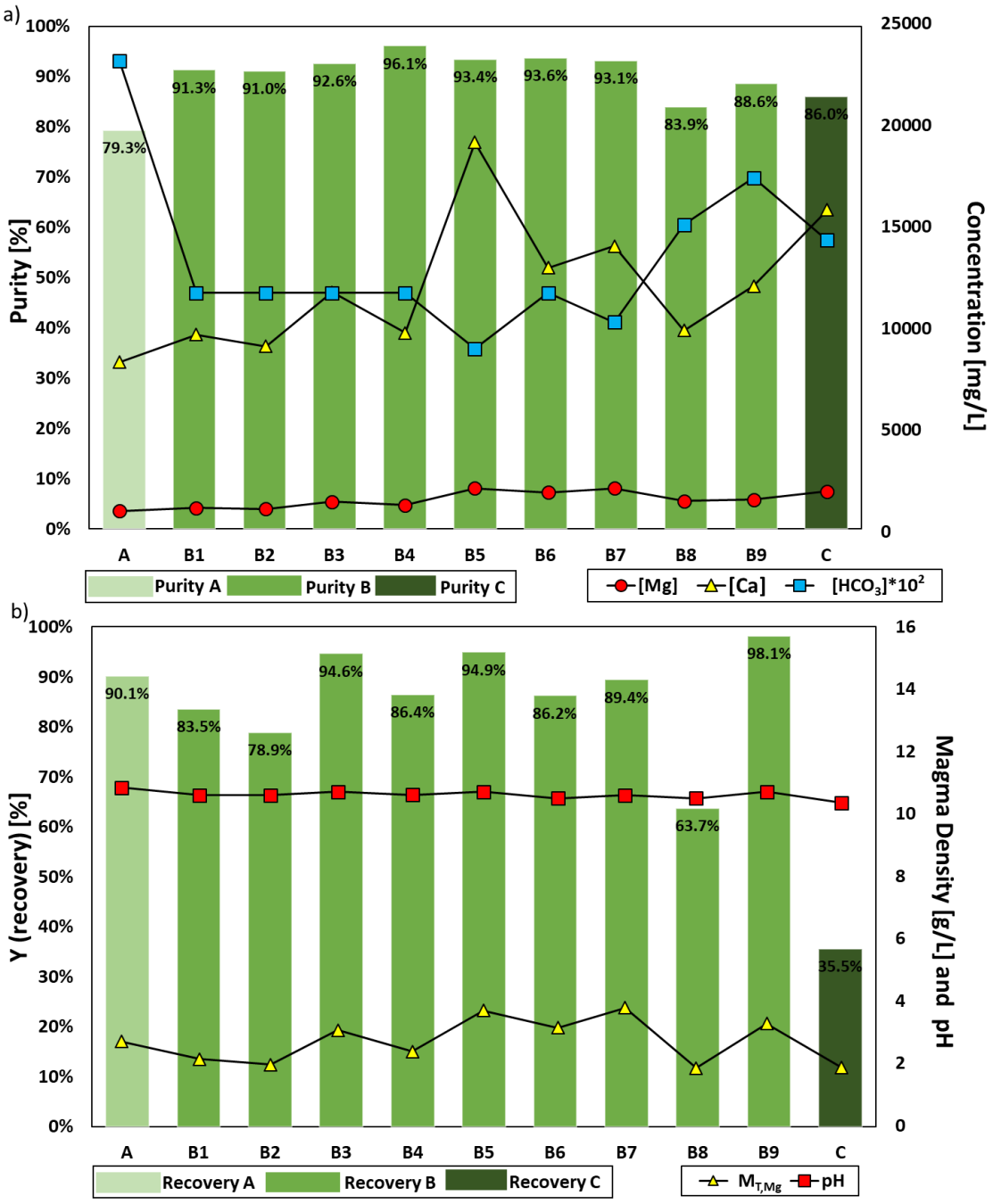

Figure 10. a) Purity of $Mg(OH)_2$ solids for all precipitation tests, accompanied by magnesium, calcium and bicarbonate concentration in the feed brine; b) Mg recovery efficiency, reaction pH and magma density.

Concerning the $Mg(OH)_2$ solids purity, IC analyses have shown that only Mg and Ca cations were present in the $Mg(OH)_2$ precipitate. The purity was typically higher than 90% for most of the tests with a peak of 96.1% for case B4, though for some tests values below 90% were found with a

minimum of 79.3% for case A. A clear influence of bicarbonates concentration on the solids purity is evident from Figure 10. In fact, in all cases, the purity was affected by the co-precipitation of calcium carbonate, as indicated by XRD analysis reported in the Supplementary Information file. In particular, calcium was found in the form of *calcite* as the most stable species at the operating conditions (10-15°C and pH of 10.5 [46]) and its precipitation can indeed be attributed to the large concentration of bicarbonate ions (HCO_3^-) in the feed brines. A theoretical analysis of precipitation equilibria performed with the Medusa software [47], is also reported in the Supplementary Information file and confirms the above findings.

The recovery efficiency was in most cases equal to or above 80%, with peaks above 95%. pH trends did not show a clear quantitative relationship with the recovery efficiency. However, the lowest values (35 % and 64%) represent tests in which lower pH values were maintained due to non-optimal control of feed flow-rate for cases B8 and C.

The magma density of the produced slurry is strictly dependent on the amount of magnesium and bicarbonate-ions in the feed brine and can be related also to magnesium recovery efficiency.

3.2.2 Calcium hydroxide precipitation step

The second precipitation step aims at the quantitative removal of all bivalent cations from the brine produced after settling and filtration of the first precipitation step, in order to make it suitable for NaCl-recovery through the rest of the treatment chain described in Figure 1. Thus, other major performance parameter is the recovery efficiency of Mg and Ca, which indicates the removal efficiency of bivalent cations from the brine.

Solid purity and recovery efficiency for both Ca and Mg are reported in Figure 11, where also magnesium and calcium concentration in the feed brine and magma density are reported to support the results.

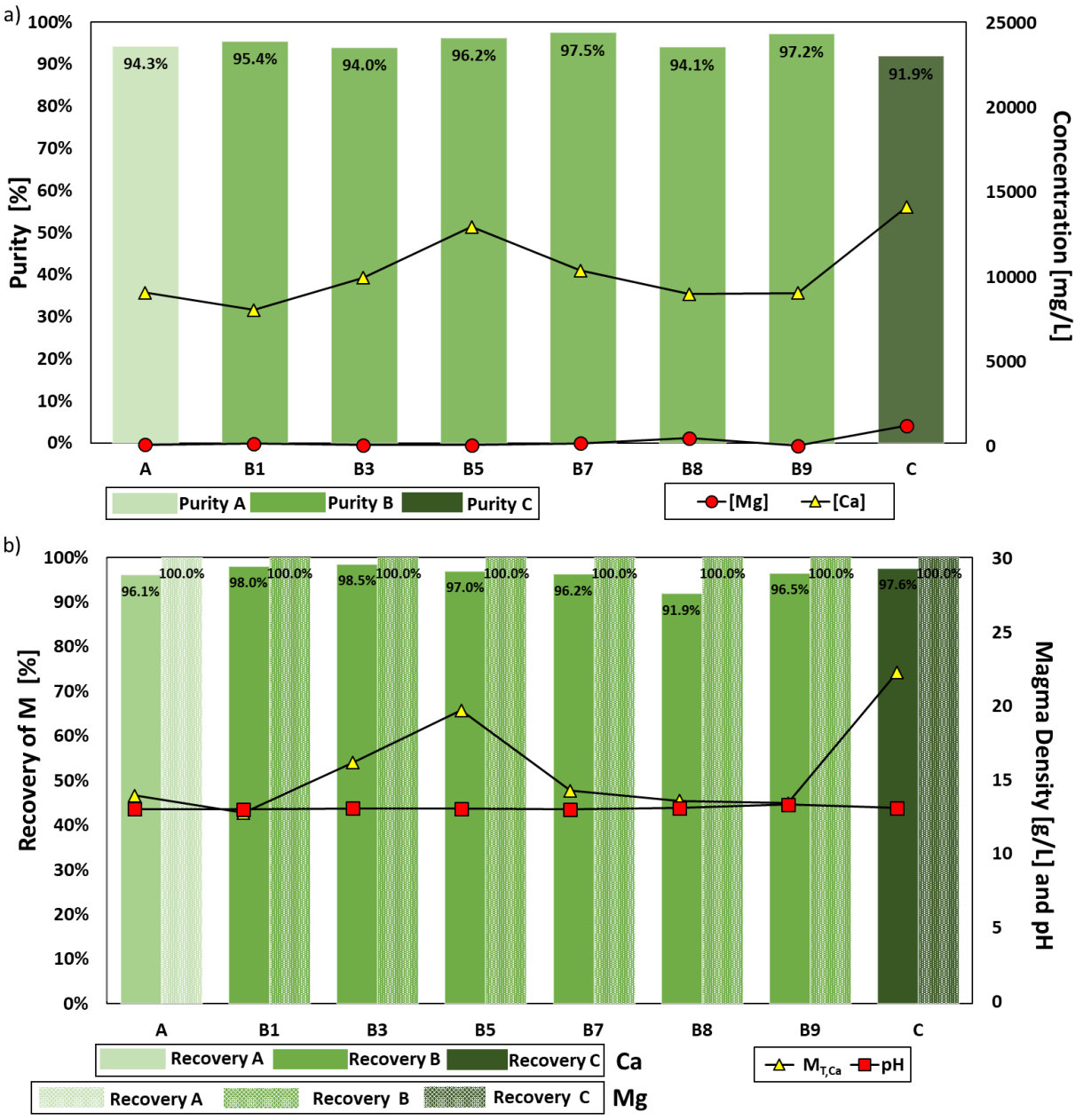

Figure 11. a) Purity of $Ca(OH)_2$ solids accompanied by magnesium and calcium concentration in the feed brine (entering the second precipitation step, after Mg recovery); b) Ca and Mg recovery efficiency, accompanied by the Magma density and reaction pH.

Also in this case, IC analyses confirmed that only Mg and Ca were present in the $Ca(OH)_2$ precipitate. The purity in Ca was around 95% for the all the tests, with a maximum value of the 97.5% for the case B7 and a minimum value of the 92% for the case C. The purity was affected by the co-precipitation of magnesium hydroxide, especially for tests with a lower Mg recovery

efficiency in the first precipitation stage. However, it is worth noting that, higher values of purity were expected (C_{Mg} in the feed brine is very low in most cases and this would affect the solid purity by about 1-2% maximum in all tests but the B8 and C, for which a very low recovery of Mg was observed in the first precipitation step), thus indicating that a problem of entrainment of magnesium hydroxide fine particles in the clarified and filtered solution used to feed the 2nd precipitation step.

Calcium removal efficiency ranged from about 92% to 98.5%, while magnesium was totally removed by precipitation, thanks to the very high pH values achieved (> 13). Thus, an overall removal efficiency of bivalent cations above 97% was reached in most cases.

Finally, the produced slurry magma density mostly followed the calcium concentration in the inlet feed brine, being that calcium is the major bivalent cation in the salt mixture.

3.3 Drum filtration for solids separation

Optimal operation of the drum filter requires a feed slurry with a minimum volume of about 100 L and a particles concentration ranging from 60 to 100 g/L, [48], high solids concentration in the feed promotes a rapid formation of the cake onto the cloth surface [48], which allows for the effective filtration of solid particles.

In order to fulfil these requirements, after each precipitation step, the produced slurry was sent into the settling tanks, *T5* and *T4*, respectively, in order to obtain a more concentrated slurry and a clarified brine. The settling phase required about 16-18 hours in order to effectively obtain a well separated clarified phase with a volume ranging from 80% to 95% of the initial slurry volume (larger values refer to the settling of magnesium hydroxide slurry). The concentrate slurry was sent to the inlet tank of the drum filter (*T8* for magnesium slurry and *T9* for calcium) and accumulated for several tests, in order to reach the volume required to properly operate the drum filter.

Solids obtained from the filtration of the collected slurries were also analysed to measure the purity, finding a value close to the average observed in all tests, i.e. around 90% for $Mg(OH)_2$ precipitate and 94% for $Ca(OH)_2$.

3.4 Outlet brine neutralization

Following the final sedimentation and filtration steps, the clarified brine together with the filtrate undergo a pH neutralization step, which is propaedeutic to the subsequent phases of the treatment chain for NaCl-solution valorization (see Figure 1). As reported in paragraph 2.2.3, the neutralization section was carried out via two consecutive steps in order to better control the obtained pH along the typical shape of a neutralization curve (Figure 12).

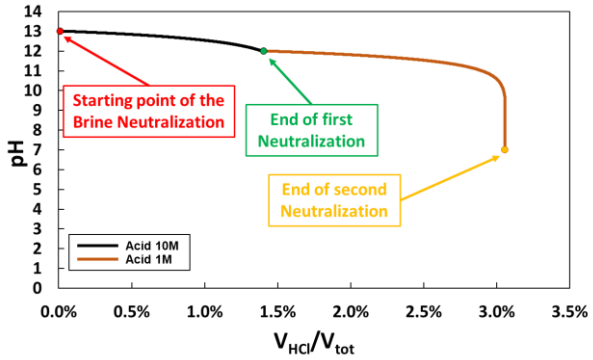

Figure 12. Conceptual description of the neutralization steps represented by the variation of pH *vs* V_{acid}/V_{tot}.

Starting from a pH value near 13 (red point), an aqueous solution of 10M hydrochloric acid (HCl) was added to the brine in order to neutralize about 90% of the hydroxyl ions, reaching a pH of near 12. After the first neutralization step, a 1M HCl solution was added in order to complete the neutralization reaching the equilibrium point (pH=7). Such step required a fine control of the acid solution volume added due to the dramatic sensitivity of pH to strong acid addition when it decreases to below 10. Very small volumes of acid solution (3% of brine volume) were needed for the neutralization of the brine, thus resulting in a final composition very similar to that obtained after the second precipitation step, as reported in Table 6.

Table 6. Average composition of the neutralized brine.

Case ID	Cation composition [g/L]				Anion composition [g/L]	
	Na^+	K^+	Ca^{2+}	Mg^{2+}	Cl^-	SO_4^{2-}
A	24.1	0.08	0.28	0.0	15.2	0.12
B	19.3 (±4.1)	0.13 (±0.04)	0.27 (±0.24)	0.0	29.0 (±10.9)	0.33 (±0.3)
C	25.3	0.18	0.28	0.0	43.3	0.49

Interestingly, the brines produced by the pilot unit were essentially free of magnesium, while calcium concentration was reduced by 97-98%, thus achieving overall a very good efficiency of bivalent cations removal, suitable for further processing if in the NaCl-solution valorisation treatment chain.

4. Conclusions

A pilot plant for the recovery and removal of bivalent cations from spent IEXs brines has been designed, built and tested with real brines, demonstrating the possibility to recover magnesium and calcium hydroxide in a fractionated way (two precipitation steps) through an accurate control of the reaction pH. The pilot plant is equipped with an unconventional proprietary (ResourSEAs SrL) reactive crystallizer named MF-PFR (Multiple Feed-Plug Flow Reactor), whose design allows an optimal distribution and mixing of the two reacting streams. A drum filter, buffer tanks and a neutralisation unit complete the pilot system, which was installed and tested within a larger treatment chain, aiming at the valorisation of spent brines, from IEXs plant via the recovery of magnesium and calcium hydroxide and the regeneration of highly concentrated NaCl solutions.

Long-run tests were carried out feeding the pilot with real industrial brines and demonstrating the plant stability and robustness. The recovered $Mg(OH)_2$ solids exhibited a purity above 90% in most cases, with a peak of 96 % and lower values around 84%. The major contaminant was calcite, coprecipitated with magnesium hydroxide due to the high concentration of bicarbonates in the feed brine. This makes the purity of recovered solids suitable for a number of market applications of magnesium hydroxide, such as flame retardant, environmental and metallurgical sectors.

Regarding the second precipitation step, the recovered $Ca(OH)_2$ solids exhibited a purity above 92% in all tests, with the second component being $Mg(OH)_2$. A Ca recovery in the form of $Ca(OH)_2$ above 95% was found, while a complete Mg removal was achieved in the second precipitation step, thus leading to an overall average removal efficiency of bivalent cations well above 97%. This makes the brine suitable for the subsequent steps of the treatment chain for the NaCl-solution valorisation.

Further developments will focus on the increase of magnesium hydroxide purity (targeting a value above 95%), by a brine pre-treatment step for removing bicarbonate ions via acidification + degassing and slightly evacuated packed column.

Moreover, the application potential of the pilot technology will be further explored by assessing the magnesium recovery performances using different feed industrial brines (e.g. desalination brines and saltworks bitterns).

Acknowledgements

This work was funded by the ZERO BRINE project (ZERO BRINE – Industrial Desalination – Resource Recovery – Circular Economy) - Horizon 2020 programme, Project Number: 730390. www.zerobrine.eu.

Authors would like to acknowledge the support of Delft University of Technology (TU-Delft) staff, in particular, Mr. Hamed Rastegarianjahromi, Dr. Amir Haidari and Prof. Henri Spanjers, for their support during the installation and testing of the pilot plant in Botlek (NL).

List of abbreviations

CRM	Critical Raw Material
TDS	Total Dissolved Solid
RO	Reverse Osmosis
FO	Forward Osmosis
PRO	Pressure Retarded Osmosis
MSF	Multi Stage Flash
MD	Membrane Distillation
MED	Multiple effect distillation
ZLD	Zero Liquid Discharge
IEXs	Ion eXchange resins softening
BMED	Bipolar Membrane Electro-Dialysis
NF	Nano-Filtration

P&ID	Piping and instrumentation diagram
PE	Polyethylene
PP	Polypropylene
PVC	Polyvinyl chloride
LLDPE	Linear low density polyethylene
HDPE	High density polyethylene
MF-PFR	Multiple Feed Plug Flow Reactor
IC	Ion Chromatography
XRD	X-Ray Diffractometry

Nomenclature

M_T	Magma density [g/l]
C	Concentration [g/l]
Y	Recovery
N_i^o	Initial mole flow rate of calcium or magnesium (mol/s)
N_i	Outlet mole flow rate of calcium or magnesium (mol/s)

5. References

[1] T.M. Missimer, R.G. Maliva, Environmental issues in seawater reverse osmosis desalination: Intakes and outfalls, Desalination. 434 (2018) 198–215. https://doi.org/10.1016/j.desal.2017.07.012.

[2] M.A. Dawoud, Environmental Impacts of Seawater Desalination: Arabian Gulf Case Study, Int. J. Environ. Sustain. 1 (2012) 22–37. https://doi.org/10.24102/ijes.v1i3.96.

[3] A. Cipollina, A. Brucato, G. Micale, A. Cipollina, A. Brucato, G. Micale, Desalination and Water Treatment A mathematical tool for describing the behaviour of a dense effluent discharge A mathematical tool for describing the behaviour of a dense effluent discharge, (2012) 37–41. https://doi.org/10.5004/dwt.2009.311.

[4] A. Cipollina, G. Micale, L. Rizzuti, A brine evaporative cooler/concentrator for autonomous thermal desalination units, Desalin. Water Treat. 31 (2011) 269–278. https://doi.org/10.5004/dwt.2011.2345.

[5] A. Cipollina, A. Misseri, G.D.A. Staiti, A. Galia, G. Micale, O. Scialdone, Integrated production of fresh water, sea salt and magnesium from sea water, Desalin. Water Treat. 49 (2012) 390–403. https://doi.org/10.1080/19443994.2012.699340.

[6] S. Casas, C. Aladjem, E. Larrotcha, O. Gibert, C. Valderrama, J.L. Cortina, Valorisation of Ca and Mg by-products from mining and seawater desalination brines for water treatment applications, J. Chem. Technol. Biotechnol. 89 (2014) 872–883. https://doi.org/10.1002/jctb.4326.

[7] European Commission, Study on the review of the list of critical raw materials. Non-critical raw materials factsheets., 2017. https://doi.org/10.2873/876644.

[8] A. Cipollina, M. Bevacqua, P. Dolcimascolo, A. Tamburini, A. Brucato, H. Glade, L. Buether, G. Micale, Reactive crystallisation process for magnesium recovery from concentrated brines, Desalin. Water Treat. 55 (2015) 2377–2388. https://doi.org/10.1080/19443994.2014.947771.

[9] M. Turek, Electrodialytic desalination and concentration of coal-mine brine, Desalination. 162 (2004) 355–359. https://doi.org/10.1016/S0011-9164(04)00069-4.

[10] M. Turek, P. Dydo, R. Klimek, Salt production from coal-mine brine in ED-evaporation-crystallization system, Desalination. 184 (2005) 439–446. https://doi.org/10.1016/j.desal.2005.03.047.

[11] M. Turek, W. Gnot, Precipitation of Magnesium Hydroxide from Brine, Ind. Eng. Chem. Res. 34 (1995) 244–250. https://doi.org/10.1021/ie00040a025.

[12] M. Micari, A. Cipollina, A. Tamburini, M. Moser, V. Bertsch, G. Micale, Techno-economic analysis of integrated processes for the treatment and valorisation of neutral coal mine effluents, J. Clean. Prod. 270 (2020) 122472. https://doi.org/10.1016/j.jclepro.2020.122472.

[13] M.O. Mavukkandy, C.M. Chabib, I. Mustafa, A. Al Ghaferi, F. AlMarzooqi, Brine management in desalination industry: From waste to resources generation, Desalination. 472 (2019) 114187. https://doi.org/10.1016/j.desal.2019.114187.

[14] E. Jones, M. Qadir, M.T.H. van Vliet, V. Smakhtin, S. mu Kang, The state of desalination and brine production: A global outlook, Sci. Total Environ. 657 (2019) 1343–1356. https://doi.org/10.1016/j.scitotenv.2018.12.076.

[15] T. Mezher, H. Fath, Z. Abbas, A. Khaled, Techno-economic assessment and environmental impacts of desalination technologies, Desalination. 266 (2011) 263–273. https://doi.org/10.1016/j.desal.2010.08.035.

[16] N. Voutchkov, Overview of seawater concentrate disposal alternatives, Desalination. 273 (2011) 205–219. https://doi.org/10.1016/j.desal.2010.10.018.

[17] T. Jeppesen, L. Shu, G. Keir, V. Jegatheesan, Metal recovery from reverse osmosis concentrate, J. Clean. Prod. 17 (2009) 703–707. https://doi.org/10.1016/j.jclepro.2008.11.013.

[18] G. Al Bazedi, R.S. Ettouney, S.R. Tewfik, M.H. Sorour, M.A. El-Rifai, Salt recovery from brine generated by large-scale seawater desalination plants, Desalin. Water Treat. 52 (2014) 4689–4697. https://doi.org/10.1080/19443994.2013.810381.

[19] R.G. Maliva, T.M. Missimer, R. Fontaine, Injection Well Options for Sustainable Disposal of Desalination Concentrate, IDA J. Desalin. Water Reuse. 3 (2011) 17–23. https://doi.org/10.1179/ida.2011.3.3.17.

[20] N. Afrasiabi, E. Shahbazali, Ro brine treatment and disposal methods, Desalin. Water Treat. 35 (2011) 39–53. https://doi.org/10.5004/dwt.2011.3128.

[21] S. Panta, P. Lane, R. Doyle, M. Hardie, G. Haros, S. Shabala, Halophytes as a Possible Alternative to Desalination Plants, Elsevier Inc., 2016. https://doi.org/10.1016/b978-0-12-801854-5.00019-4.

[22] A. Panagopoulos, K.J. Haralambous, M. Loizidou, Desalination brine disposal methods and treatment technologies - A review, Sci. Total Environ. 693 (2019) 133545. https://doi.org/10.1016/j.scitotenv.2019.07.351.

[23] P. Xu, T.Y. Cath, A.P. Robertson, M. Reinhard, J.O. Leckie, J.E. Drewes, Critical review of desalination concentrate management, treatment and beneficial use, Environ. Eng. Sci. 30 (2013) 502–514. https://doi.org/10.1089/ees.2012.0348.

[24] B.K. Pramanik, L. Shu, V. Jegatheesan, A review of the management and treatment of brine solutions, Environ. Sci. Water Res. Technol. 3 (2017) 625–658. https://doi.org/10.1039/c6ew00339g.

[25] A. Subramani, J.G. Jacangelo, Treatment technologies for reverse osmosis concentrate volume minimization: A review, Sep. Purif. Technol. 122 (2014) 472–489. https://doi.org/10.1016/j.seppur.2013.12.004.

[26] A. Giwa, V. Dufour, F. Al Marzooqi, M. Al Kaabi, S.W. Hasan, Brine management methods: Recent innovations and current status, Desalination. 407 (2017) 1–23. https://doi.org/10.1016/j.desal.2016.12.008.

[27] J.R. McCutcheon, R.L. McGinnis, M. Elimelech, Desalination by ammonia-carbon dioxide forward osmosis: Influence of draw and feed solution concentrations on process performance, J. Memb. Sci. 278 (2006) 114–123. https://doi.org/10.1016/j.memsci.2005.10.048.

[28] R.L. McGinnis, M. Elimelech, Energy requirements of ammonia-carbon dioxide forward osmosis desalination, Desalination. 207 (2007) 370–382. https://doi.org/10.1016/j.desal.2006.08.012.

[29] Y. Kim, J.H. Lee, Y.C. Kim, K.H. Lee, I.S. Park, S.J. Park, Operation and simulation of pilot-scale forward osmosis desalination with ammonium bicarbonate, Chem. Eng. Res. Des. 94 (2015) 390–395. https://doi.org/10.1016/j.cherd.2014.08.015.

[30] N. Bajraktari, C. Hélix-Nielsen, H.T. Madsen, Pressure retarded osmosis from hypersaline sources — A review, Desalination. 413 (2017) 65–85. https://doi.org/10.1016/j.desal.2017.02.017.

[31] O.K. J.Gilron, Y. Folkman, R. Savliev, M. Waisman, WAIV - wind aided intensified evaporation for reduction of desalination brine volume, Desalination. 158 (2003) 205–214.

[32] H. Bamufleh, F. Abdelhady, H.M. Baaqeel, M.M. El-Halwagi, Optimization of multi-effect distillation with brine treatment via membrane distillation and process heat integration, Desalination. 408 (2017) 110–118. https://doi.org/10.1016/j.desal.2017.01.016.

[33] F. Laganà, G. Barbieri, E. Drioli, Direct contact membrane distillation: modelling and concentration experiments, J. Memb. Sci. 166 (2000) 1–11.

[34] D. Brogioli, F. La Mantia, N.Y. Yip, Thermodynamic analysis and energy efficiency of thermal desalination processes, Desalination. 428 (2018) 29–39. https://doi.org/10.1016/j.desal.2017.11.010.

[35] I.S. Al Mutaz, K.M. Wagialia, Production of magnesium from desalination brines, Resour. Conserv. Recycl. 3 (1990) 231–239. https://doi.org/10.1016/0921-3449(90)90020-5.

[36] P.S. Wallace, D4_WO2015077727A1.pdf, PCT/US2014/067176, n.d.

[37] H.R. Flodman, B.I. Dvorak, Brine Reuse in Ion-Exchange Softening: Salt Discharge, Hardness Leakage, and Capacity Tradeoffs, Water Environ. Res. 84 (2012) 535–543. https://doi.org/10.2175/106143012x13373550427354.

[38] Y. Chen, J.R. Davis, C.H. Nguyen, J.C. Baygents, J. Farrell, Electrochemical Ion-Exchange Regeneration and Fluidized Bed Crystallization for Zero-Liquid-Discharge Water Softening, Environ. Sci. Technol. 50 (2016) 5900–5907. https://doi.org/10.1021/acs.est.5b05606.

[39] M. Micari, A. Cipollina, A. Tamburini, M. Moser, V. Bertsch, G. Micale, Combined membrane and thermal desalination processes for the treatment of ion exchange resins spent brine, Appl. Energy. 254 (2019) 113699. https://doi.org/10.1016/j.apenergy.2019.113699.

[40] M. Micari, M. Moser, A. Cipollina, A. Tamburini, G. Micale, V. Bertsch, Towards the implementation of circular economy in the water softening industry: A technical, economic and environmental analysis, J. Clean. Prod. 255 (2020) 120291. https://doi.org/10.1016/j.jclepro.2020.120291.

[41] M. Bevacqua, F. Vassallo, A. Cipollina, G. Micale, A. Tamburini, M. Papapetrou, F. Vicari, Reattore e processo di precipitazione di un prodotto solido, Application IT 102021000012473, 2021.

[42] P.S. Forms, Horizon 2020 Call : H2020-IND-CE-2016-17 (Industry 2020 in the Circular

Economy) Topic : CIRC-02-2016-2017 Type of action : IA (Innovation action) Proposal number : 730209-1 Proposal acronym : Renut Deadline Id : H2020-CIRC-2016TwoStage Table of conte, (2017). https://doi.org/10.1051/0004-6361:20021389.

[43] WesTech, IO&M Manual Pilot Drum Filter, (n.d.).

[44] F. Buchholtt, M.K.I. Mmelt, Self-tuning Control of a pH-Neutralization Process, Automatica. 15 (1979) 665–671.

[45] P. Chemicals, M.C. Pvc, P.F.A. Epdm, Chemical resistance guide, (2008).

[46] C.Y. Tai, F.B. Chen, Polymorphism of CaCO3 precipitated in a constant-composition environment, AIChE J. 44 (1998) 1790–1798. https://doi.org/10.1002/aic.690440810.

[47] https://www.kth.se/che/medusa/downloads-1.386254, (n.d.).

[48] D. Grasso, D. Grasso, Bioprocess Engineering Principles, 2018. https://doi.org/10.1201/9780203752265-5.

1. Supplementary Material for the article

A pilot-plant for the selective recovery of magnesium and calcium from waste brines

F. Vassallo[a], D. La Corte[a], N. Cancilla[a], A. Tamburini[a,b], M. Bevacqua[b], A. Cipollina*[a,b], G. Micale[a,b]

[a]*Dipartimento di Ingegneria, Università degli Studi di Palermo (UNIPA)- viale delle Scienze Ed.6, 90128 Palermo, Italy.*

[b]*ResourSEAs SrL, viale delle Scienze Ed.16, 90128 Palermo, Italy.*

*corresponding author: andrea.cipollina@unipa.it

Chemical equilibrium between carbonate/bicarbonate and water

The bicarbonate/carbonate ions are involved in chemical equilibrium reactions together with water [46], as in the following:

$$CO_{2(g)} \Leftrightarrow CO_{2(l)} \quad \textbf{(S1)}$$

$$CO_{2(l)} + H_2O \Leftrightarrow H_2CO_3 \quad \textbf{(S2)}$$

$$H_2CO_3 + H_2O \Leftrightarrow HCO_3^- + H_3O^+ \quad \textbf{(S3)}$$

$$HCO_3^- + H_2O \Leftrightarrow CO_3^{2-} + H_3O^+ \quad \textbf{(S4)}$$

When the pH increases above 10, chemical equilibria are shifted leading to the total conversion of dissolved CO_2 and bicarbonate ions into carbonates.

XRD analysis of magnesium hydroxide

Results of XRD analysis of magnesium hydroxide samples from all different test-runs are reported in **Figure S13**. It indicates that calcium was found in the form of *calcite* as the most stable species at the operating conditions.

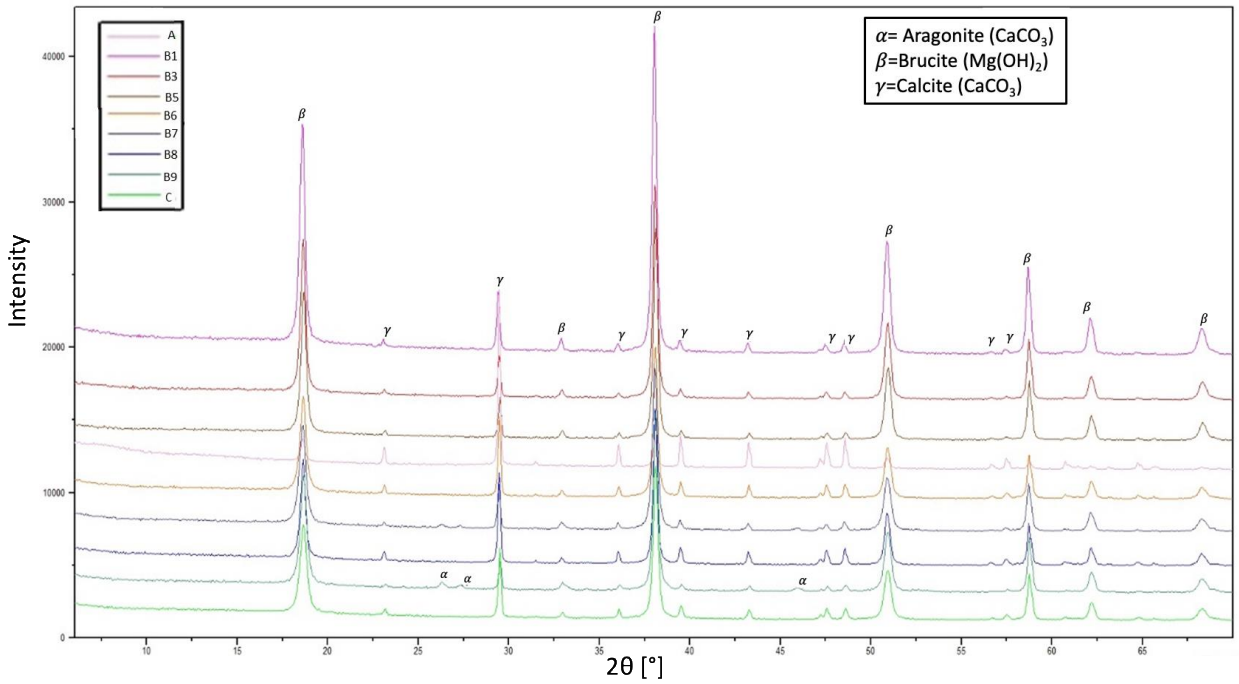

Figure S13.Cumulative XRD patterns for magnesium hydroxides samples from all different test-runs.

<u>Use of Medusa software for the prediction of chemical equilibrium and precipitation of magnesium hydroxide</u>

The MEDUSA software [44], along with the hydro-chemical equilibrium-constant database (HYDRA) was used to better understand the presence of the co-precipitated $CaCO_3$ in $Mg(OH)_2$ solids.

The required input needed to run the simulation are: (i) temperature at which the precipitation occurs and (ii) molar concentration of the ions.

Figure S1 shows the results of the simulation carried out considering the average composition of case B (Std, reported in Table 3).

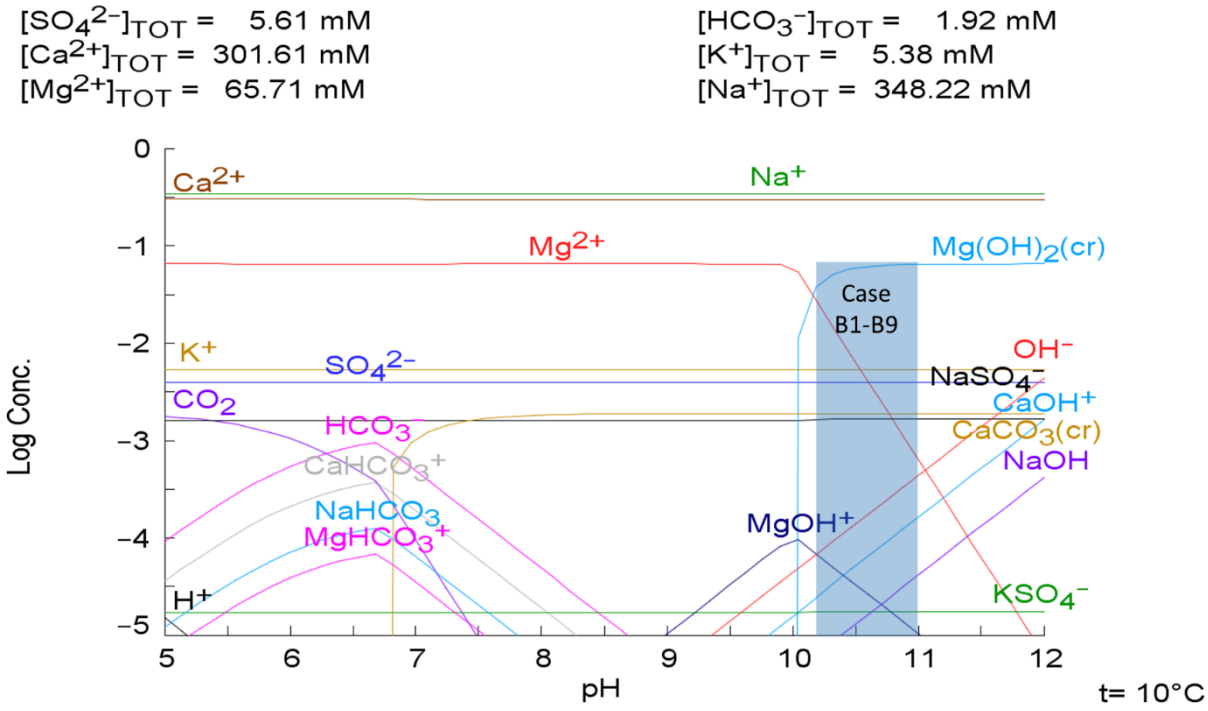

Figure S14. pH versus log concentration plot for the case A at 10°C, fixing the [Na^+]=0.348M (8.01 g/l), [Mg^{2+}]=0.66M (1.60g/l), [Ca^{2+}]=0.30M (12.1 g/l), [SO_4^{2-}]=0.0056M (0.54g/l) and [HCO_3^-]= 0.0019M (0.12g/l).

As shown in **Figure S14**, at the pH value of the tested brines grouped in case B (varying between 10.35 and 10.8), predictions confirm that recovery increases from 81% at pH equal to 10.35 (case B8, experimental conversion equal to 84%), up to 98% at a pH of 10.8 (case B9, experimental conversion equal to 98%).